Study of the effect of different synthesis routes on Li extraction-insertion from $LiCoPO_4$

Natalia N. Bramnik*, Kirill G. Bramnik, Carsten Baehtz, Helmut Ehrenberg

Institute of Materials Science,
University of Technology Darmstadt,
D-64287, Darmstadt, Germany

Tel.: +49 (6151) 166359
Fax: +49 (6151) 166377
e-mail: bramnik@tu-darmstadt.de

Abstract

The electrochemical performance of $LiCoPO_4$-based electrodes was studied in dependence on synthetic conditions. The role of particle size distribution is illustrated. Structural changes occurring at lithium extraction-insertion was explored by ex-situ and in-situ synchrotron XRD measurements. For the samples annealed at temperature lower than 600°C the amorphisation of the cathode material was identified. For a high-temperature sample the two-phase character of electrochemical reaction was confirmed. The character of structural changes observed at charge and discharge is different: the two-phase reaction $LiCoPO_4$-"$CoPO_4$" occurs during charging, while discharge induces a strong increase of the cell volume for the Li-poor phase.

Keywords

Phospho-olivine, lithium batteries, in situ diffraction, synchrotron

*Corresponding author

1. Introduction

Metallophosphates $LiMePO_4$ (Me = Fe, Co, Mn, Ni) with olivine-type structure have attracted a strong attention in the last years as perspective intercalation materials for lithium-ion batteries [1, 2, 3]. This interest is focused mostly on the lithium iron phosphate because of the favorite discharge voltage (ca 3.6 V vs. metallic lithium) and the environmental compatibility of iron. Different approaches for enhancing of the electrochemical performance of this compound were described [4-6]. The key points were shown to be a small particle size and good electronic contact between the particles of the sample.

The mechanism of lithium extraction-insertion from $LiFePO_4$ is properly identified with ex-situ and in-situ X-ray diffraction, Mössbauer spectroscopy as well as electrochemical techniques [1, 7, 8]. As the lithium extraction from $LiFePO_4$ (tryphylite) proceeds, the new phase $FePO_4$ (heterosite) is formed. Both phases are isostructural (space group *Pnma*) with slight difference in the cell parameters. The two-phase character of the reaction seems to provoke low rate capability of this compound due to the hindered lithium diffusion through the $LiFePO_4/FePO_4$ interface [1].

In contrast to $FePO_4$ with olivine-type structure, the existence of $CoPO_4$ and $MnPO_4$ crystallizing in the same space group is still not proved. Nevertheless, a two-phase mechanism of lithium deinsertion from $LiMnPO_4$ and $LiCoPO_4$ seems to take place also [9-12]. According to Li et al., the second phase arising by the lithium extraction from lithium manganese phosphate has a composition Li_xMnPO_4, where x is very close to zero [9]. Recently, Delacourt et al. showed that the electrochemical delithiation of $LiMnPO_4$, prepared by a new precipitation route, leads to the disappearing of pristine $LiMnPO_4$ and to the formation of the new phase with the same structure, but with lower cell volume (302 $Å^3$ and 275 $Å^3$, respectively) [10]. The authors suggest that the appearing phase is $MnPO_4$.

Previously, we have shown that $LiCoPO_4$-samples prepared by solid-state reaction at high temperature demonstrate unsatisfactory electrochemical performance [13]. The reversibility of

lithium extraction-insertion from $LiCoPO_4$ was improved by a synthetic approach based on the precursor $NH_4CoPO_4 \bullet H_2O$ [14], although the capacity fading during cycling was still very pronounced. At the same time, both samples seem to show a different behavior during lithium deintercalation. The peak splitting in the diffraction pattern, observed for the high temperature sample, pointed out the two phase character of the electrochemical reaction. We analyzed diffraction pattern of Li_xCoPO_4-sample charged to x=0.05 (from the electrochemical data) by refining a two-phase model with the same space group [13]. The difference in the cell volumes for both phases was found to be much lower (283.5 $Å^3$ and 278.4 $Å^3$, respectively) in comparison with the data reported for manganese metallophosphate. For $LiCoPO_4$ prepared by the "precursor-method", strong amorphisation of the sample during the charging could be identified only.

In this paper, we studied electrochemical extraction of lithium from $LiCoPO_4$ with *ex-situ* and *in-situ* X-ray diffraction and propose that lithium extraction proceeds in different ways in dependence from particle size.

2. Experimental

$LiCoPO_4$ was prepared by solid-state reaction of stoichiometric amounts of CoO, Li_2CO_3 and $(NH_4)_2HPO_4$ (referred in following as "direct synthesis"). Carbon black (5 % weight) was added to the reactants to minimize particle size during the synthesis and provide better electronic contact between the $LiCoPO_4$-particles. The components were dispersed into acetone, ground together in an agate mortar, pressed into a pellet and calcined at 500°C for 12 hours in N_2-flow. After additional grinding and pelletizing, the mixture was hold 24 hours in nitrogen atmosphere at different temperatures (600°C and 800°C, respectively). The final product contains 7.2% weight carbon. $LiCoPO_4$ samples were also prepared from a NH_4CoPO_4-precursor obtained as described [14] by the reaction with a stoichiometric amount

of Li_2CO_3 at different temperatures ("precursor synthesis"). In this case the reaction was performed in air without any adding of carbon black.

Scanning electron microscope Philips XL 30 FEG was used to observe the particle morphology. To measure the surface area of powders the BET method was used (Autosorb 3B, QuantaChrome). Electrochemical studies were carried out with a multichannel potentiostatic-galvanostatic system VMP (Perkin Elmer Instruments, USA). Swagelok-type cells were assembled in argon-filled dry box with water and oxygen contents less than 1 ppm. The cathode composite was fabricated as follows: 70% active material, 25% acetylene carbon black and 5% polyvinylidene fluoride as polymer binder were intimately mixed, ground in an agate mortar and pressed onto an Al-mesh (resulting electrodes contain about 3 mg of active compound). In situ synchrotron measurements were made with the electrochemical cell developed in our laboratory [15]. The cell operating in transmission mode is a coin-cell type with an overall thickness below 1 mm along the beam path. It consists of lithium anode, glass-fiber separator soaked with electrolyte Selektipur-31 (Merck, Germany, 1M $LiPF_6$ in EC:DMC-2:1 vol. %) and cathode pressed into a pellet. The stainless steel anode support and aluminum cup at the beam entrance window serve as current collectors. The cell is mounted on a flat sample holder which can be oscillated to reduce preferred orientation effects in powder statistics. The on-site readable image-plate detector "OBI" [16] collects the whole diffraction pattern with a high time resolution (about 60 patterns per charge). Structure characterization was performed by Rietveld analysis using the Winplotr software package [17].

During in situ measurements the cell was charged and discharged galvanostatically with a current of 0.2 mA (close to C/18). The samples for ex situ measurements were prepared in Swagelok cells and characterized using a STOE STADI/P powder diffractometer ($MoK\alpha_1$ radiation, curved Ge (111) monochromator, transmission mode, step 0.02° (2θ), linear PSD counter).

3. Results and Discussion

Both samples prepared by "direct synthesis" at 800°C and 600°C were found to be single-phase $LiCoPO_4$ with an ordered olivine structure indexed by orthorhombic *Pnma* with a cell volume of 283.58(2) $Å^3$ based on XRD data. The samples synthesized from the precursor $NH_4CoPO_4 \cdot H_2O$ contained $LiCoPO_4$ as a main product and Co_3O_4 as an admixture. The amount of admixtures did not exceed 5 weight %.

3.1. Electrochemical characterization

The cathode performance evaluated galvanostatically at C/1.5 depends significantly on the sintering temperature (Fig.1). For the $LiCoPO_4$ prepared at 800°C charge and discharge capacities are significantly lower even at higher inversion potential in comparison with the sample prepared at 600°C. Moreover, the lithium extraction-insertion proceeds with higher polarization. This fact is not surprising and results apparently from the difference in particle size distribution. Lower temperature of synthesis is favorable for the formation of smaller particles, which are preferable for olivine-like metallophosphates with low ionic and electronic conductivity. Decreasing the rate to C/6 could enhance the discharge capacity in the first cycle up to 102 $mAh \cdot g^{-1}$. This value is very close to the data reported for this compound by Okada et al [12].

To confirm the role of particle size, we applied ball-milling for 15 minutes to the cathode mixture of the sample prepared at 800°C. After ball-milling we obtained better pronounced charge-discharge curves and smaller polarization in the system (Fig.1). Nevertheless the electrochemical performance is still poorer than for the sample prepared at 600°C. Prolonged ball-milling (up to 2 hours) provided no further improvement of the cathode properties.

The comparison of morphology of the samples prepared at different temperatures shows that electrochemical performance is in good agreement with particle size distribution (Fig.2). The big crystallites (around 5-10 μm) observed for high temperature sample were not identified

after ball-milling of the sample. For the sample prepared at 600°C particle size does not exceed 1-2 μm and this sample has the best electrochemical performance.

Additional treatment did not result in any improvement of the electrochemical performance of the $LiCoPO_4$-cathode. First, the following ball-milling of the sample annealed at 600°C did not enhance discharge capacity significantly. Second, using "precursor" synthetic way, we could decrease the temperature of synthesis down to 350°C in order to get smaller particles. The electrochemical behavior of the samples prepared by "precursor" synthesis with and without adding carbon black was the same. Fig. 3 illustrates the charge-discharge curves for the samples, obtained by "precursor" method at different temperatures. The polarization of the cell decreases with decreasing of annealing temperature. Moreover, BET measurements indicate a specific surface area of 11.9 $m^2 \cdot g^{-1}$ for the sample annealed at 350°C and 3.4 $m^2 \cdot g^{-1}$ for the sample annealed at 600°C. These facts can be taken as indication that average particle size becomes smaller with the decrease of the synthetic temperature. Nevertheless, the capacity loss in the first cycle is still very high. Probably, the following decrease of particle size provokes stronger electrolyte decomposition, so that the enhancement of the electrochemical performance through increase of cathode active surface area is not possible. At the same time, the contribution of electrolyte decomposition seems to be more pronounced during cycling at lower current rate (see Fig.4). Indeed, up to current density corresponding C/4.5 discharge capacity increases as well as charge capacity. This common behaviour results usually from the limited kinetic of lithium transport. Simultaneously, polarization in the cell decreases in this range. Beginning from current density C/6 discharge capacity decreases and consists at C/20 of about 25 mA/g. At low current density charging the cell takes more time, so that the electrolyte decomposition is stronger.

The maximal discharge capacity (100 mAh/g) for the sample annealed at 500°C was achieved at current density C/4.5. Even in this case the difference between charge and discharge capacity is very high, so the capacity loss in the first cycle is about 35%. It was already

mentioned, the electrolyte decomposition upon charge can contribute to this capacity loss. Indeed, the crucial role of electrolyte was pointed out in a recent study [18]. The significant improvement of capacity retention of $LiCoPO_4$-cells with $LiBF_4$-based electrolyte was reported. On the other hand, in case of two-phase reaction the difference in lithium mobility in pristine and delithiated phase can contribute to the difference between charge and discharge capacity. It is interesting to note, the calculated lithium diffusion coefficients differ for $LiCoPO_4$ (10^{-9} cm^2/s) and "$CoPO_4$" (10^{-5} cm^2/s) [19].

The charge curve for the sample prepared by "direct synthesis" at 600°C (Fig.1) consists of two sub-plateaus. For the $LiCoPO_4$-samples prepared from ammonium cobalt phosphate this behavior was reported in our recent study [12] and is confirmed here (Fig.3). Moreover, a recent study from Nakayama et al. confirmed, that Li extraction reaction from $LiCoPO_4$ occurs in a two-step manner [20]. The reason of this behavior remained unclear. The authors proposed, that the second plateau is due to an increase in electrochemical polarization around $x = 0.3$. The stepwise character of lithium deinsertion was confirmed by XAS measurements.

The samples prepared through "direct synthesis" were cycled in potentiostatic mode. Conducting PITT-measurement at the accelerating current close to C/13, we found that the discharge plateau consists of two sub-plateaus, too (Fig.5a, b). Additionally, for both samples annealed at 600°C and 800°C (with additional ball-milling) the difference between the two plateaus becomes more distinct in the second and following cycles. For the sample prepared at 600°C the two step character of Li extraction/insertion can be clearly identify in the first cycle.

It has already been shown that lithium extraction occurs at both plateaus during charging [13, 20]. Consequently, the two step origin of lithium insertion/extraction from $LiCoPO_4$ is an intrinsic property of this compound and cannot be ascribed to a side reaction (electrolyte decomposition, electrochemical reaction with Al-current collector etc.). The first plateau seems to be more pronounced for samples with smaller particle size (Fig.3) and for cycling at

small current density (Fig.4). Therefore, the appearance of two plateaus might result from the kinetics of lithium extraction-insertion.

On the other hand, recent studies of $LiCoPO_4$-based thin-film electrodes reveal no two step-character of lithium extraction-insertion [18, 21]. The cyclic voltammograms obtained were characteristic for a one-step electrochemical reaction. Thus, lithium extraction character seems to depend on the real structure of the cathode material.

3.2. Ex-situ XRD characterization

3.2.1. "Direct synthesis" 800°C, ball-milling

For ex-situ characterization we prepared the samples by charging the cell to the composition $Li_{0.5}CoPO_4$ and $Li_{0.05}CoPO_4$ (as follows from the charge passed through the cell). As shown in Fig.7, the diffraction pattern of the $Li_{0.5}CoPO_4$ sample can be refined based on the two-phase structure model. This is consistent with the previously reported mechanism of lithium extraction from $LiCoPO_4$, including formation a "lithium-poor phase", which is isostructural to $LiCoPO_4$, but with a smaller cell volume ($LiCoPO_4$ –283.56(9) $Å^3$, "$CoPO_4$ – 278.36(8) $Å^3$) [13]. The weight fractions of $LiCoPO_4$ and $CoPO_4$ were found to be of 56(2)% and 44(2)%, respectively. The diffraction pattern of the charged sample $Li_{0.05}CoPO_4$ is characteristic for a one-phase system. Rietveld refinement confirmed that the crystalline phase obtained in the charged sample is lithium-poor phase only. During charging, a good agreement between phase ratios calculated from electrochemical data and the results of refinements is obtained.

Discharging the cell to 3.5 V we obtained a 50 $mAh \cdot g^{-1}$ discharge capacity (insertion of $x \sim 0.3$). If lithium extraction is reversible, the diffraction pattern should contain the reflections of both phases $LiCoPO_4$ and "$CoPO_4$", expecting weight fractions of 35% and 65% respectively. Surprisingly, no splitting of reflexes can be identified in discharged state and the diffraction

pattern is characteristic for one-phase $LiCoPO_4$. This discrepancy is unexpected and remains unexplained.

3.2.2. "Direct synthesis" 600°C

Only small amounts of the crystalline "$CoPO_4$" phase were observed, when a sample, annealed at 600°C, was charged to the composition $Li_{0.05}CoPO_4$ (Fig.8). A two-phase refinement gives weight fractions for $LiCoPO_4$ and $CoPO_4$ of 85% and 15%, respectively. This sample seems to contain a significant amorphous fraction and crystalline $LiCoPO_4$. In our opinion, lithium deintercalation from the low-temperature sample leads to an amorphisation of the cathode material. A similar behavior was recently reported by us for the sample prepared from NH_4CoPO_4-precursor and annealed at 600°C [13]. This was observed for "precursor synthesis" samples in this study too. Consequently, the amorphisation of the cathode material is more pronounced for smaller particle sizes as obtained at lower temperature. Accordingly, the very small amount of crystalline "$CoPO_4$" as observed in the diffraction pattern would correspond to some big crystallites of the sample.

3.3. In-situ XRD characterization (*"Direct synthesis" 800°C, ball-milling*)

To check the conclusions from *ex-situ* data, obtained for the high-temperature sample, we recorded X-ray diffraction data *in-situ* using synchrotron radiation. The electrochemical cell was charged to the composition $Li_{0.29}CoPO_4$ and then discharged to the composition $Li_{0.57}CoPO_4$, calculated from the electrochemical data. The evolution of the diffraction patterns during charge-discharge is shown in Fig. 9. The appearance of the second olivine-type phase during charging is illustrated here by appearing twice (020) and (301) reflections at slightly different diffraction angles 2θ due to slightly different cell parameters for both phases.

The data collected during in-situ measurements were analyzed by Rietveld refinement. Observed, calculated pattern and their difference for the cell charged to the composition $Li_{0.5}CoPO_4$ are illustrated in Fig. 10 as an example. Besides of reflections from two olivine-like phases, the strong reflections from the Al-plunger (cathode current collector) and the Li anode can be identified. Additionally, weak reflections come from an undefined phase, which can be indexed, based on have cubic face-centered cell (a = 8.56 Å). These additional peaks are always observed for this in situ cell and, therefore, assigned to the experimental setup. For all non-olivine phases observed by in situ measurements profile matching was applied.

The results of refinement are illustrated in Fig 11, 12. No visible changes on the diffraction pattern were observed until 0.1 Li was deintercalated, so that the one-phase structure model ($LiCoPO_4$) at this stage was used (see Fig.12). This region corresponds to the first peak in the incremental capacity plot for this sample. Beginning with the 12th diffractogram (composition $Li_{0.88}CoPO_4$) the second phase is visible due to appearing new reflections. The parameters for the second phase "$CoPO_4$" was refined for 22 diffractions pattern (composition $Li_{0.76}CoPO_4$) based on the structure model used for ex-situ samples and then kept constant in the composition range Δx = 0.88-0.76 in Li_xCoPO_4. Because of the small amount of the $CoPO_4$-phase in this composition range the refinement of the cell parameters might result in wrong interpretations. The same strategy for the refinement was applied for the following diffractogramms from composition $Li_{0.76}CoPO_4$. Only scale factors, U, W-parameters (equal for both phases), cell constants and background points were refined as free parameters.

The cell volumes for both phases are decreasing slightly during charging. During discharge the cell volume of the "$CoPO_4$" phase was increasing abrupt as well as the weight ratio of this phase. Thus, the cell volume of the "lithium-poor phase" was approaching the cell volume of $LiCoPO_4$. At the same time, the cell constants of "$CoPO_4$" were found to become closer to the parameters of $LiCoPO_4$ phase. The structural changes occurring also during charging and

discharging are quite different. This behavior is consistent with results of ex-situ XRD measurements, where only $LiCoPO_4$ phase can be identified in fully discharged state.

4. Conclusions

In our previous work we found that $LiCoPO_4$-samples prepared by "direct" solid state reaction show insufficient electrochemical performance. Here we have shown that the cathode properties of $LiCoPO_4$ can be improved by additional ball-milling of the sample or by the decreasing synthetic temperature. This improvement is assigned to the smaller particle size. Nevertheless, the decrease of particle size seems to provoke stronger negative influence on the decomposition of electrolyte.

The lithium extraction has a two-step character as well as lithium reinsertion. The study of the lithium extraction mechanism by X-ray diffraction is hindered due to the amorphisation of the cathode material if the particle size is small ($\leq \sim 1$ μm). For the sample annealed at high temperature 800°C with following ball-milling, the two-phase mechanism of lithium extraction was confirmed with ex-situ and in-situ XRD-measurements. The character of structural changes observed at charge and discharge is different: the two-phase reaction $LiCoPO_4$ –"$CoPO_4$" takes place during charging, while discharge induces a strong increase of the cell volume for the Li-poor phase.

Acknowledgment

This work was supported by the *Deutsche Forschungsgemeinschaft (DFG)* in the frame of SFB 595. Authors thank Prof. Dr. H. Fuess for valuable discussions.

Figure captions

Fig.1. Galvanostatic charge-discharge curves for $LiCoPO_4$-based cathodes at rate C/1.5. $LiCoPO_4$ was prepared by "direct" synthesis.

Fig.2. SEM micrograph showing the morphology of samples: a) annealed at 800°C, b) cathode mixture of the sample annealed at 800°C after ball-milling, c) annealed at 600°C. The whole section corresponds to an area of about 30μm×45 μm.

Fig. 3. First charge-discharge cycle for $LiCoPO_4$ prepared by "precursor" synthesis at different annealing temperatures (current rate close to C/1.5).

Fig.4. Rate capability of $LiCoPO_4$-cell a("precursor" synthesis, annealed at 500°C).

Fig. 5. E=f(t) curves obtained in potentiostatic mode at accelerating current close to C/13, a) $LiCoPO_4$-600°C b) $LiCoPO_4$-800°C, ball milled. Both samples were prepared by "direct synthesis".

Fig.6. Incremental capacity plot for $LiCoPO_4$ annealed at 800°C and ball-milled with carbon and PVdF for 15 minutes.

Fig.7. Ex-situ X-ray diffraction of the Li-deintercalated samples prepared from the $LiCoPO_4$ annealed at 800°C and ball-milled with carbon and PVdF for 15 minutes.

Fig. 8. X-ray diffraction pattern of the $Li_{0.05}CoPO_4$ sample ("direct" synthesis 600°C). Weight fractions of $LiCoPO_4$ and "$CoPO_4$" phase are 85% and 15%, respectively.

Fig. 9. Evolution of diffraction pattern during charge-discharge of the Li_xCoPO_4cell ($LiCoPO_4$ annealed at 800°C and ball-milled with carbon and PVdF).

Fig.10. Synchrotron X-ray diffraction pattern taken in situ for $Li_{0.5}CoPO_4$ ($\lambda = 0.70829$ Å).

Fig. 11. Change in the phase ratios during charge-discharge, calculated from refinement versus electrochemical data.

Fig. 12. Evolution of the cell parameters during charge-discharge of $LiCoPO_4$.

References

[1] A.K. Padhi, K.S. Nanjundaswamy, J.B. Goodenough, J. Electrochem. Soc., 144 (1997) 1188-1194.

[2] O. Garsía-Moreno, M. Alvares-Vega, F. Garsía-Alvarado., J. Garsía-Jaca., J.M. Gallardo-Amores, M.L. Sanjuán, U. Amador, Chem. Mater., 13 (2001) 1570-1576.

[3] A. Yamada, M. Hosoya, S-C. Chung, Y. Kudo, K. Hinokuma, K.-Yu Liu, Y. Nishi, J. Power Sources, 119-121 (2003) 232-238.

[4] A. Yamada, S-C. Chung, Y. Kudo, K. Hinokuma, J.Electrochem. Soc., 148 (2001) A224-A229.

[5] H. Huang, S.-C. Yin, L.F. Nazar, Electrochem. Solid-State Lett., 4 (2001) A170-A172.

[6] S. Franger, F. Le Gras, C. Bourbon, H. Rouault, Electrochem. Solid-State Lett., 5 (2002) A231-A233.

[7] A. Andersson, B. Kalska, L. Häggström, J. Thomas, Solid State Ionics, 130 (2000) 41-52.

[8] M. Takahashi, S. Tobishima, K. Takei, Y. Sakurai, Solid State Ionics, 148 (2002) 283-289.

[9] G. Li, H. Azuma, M. Tohda, Electrochem Solid-State Lett., 5 (2002) A135-A137.

[10] C. Delacourt, P. Poisot, M. Morcrette, J.M. Tarascon, C. Masquelier, Chem. Mater., 16 (2004), 93-99.

[11] K. Amine, H. Yazuda, M. Yamachi, Electrochem. Solid State Lett,. 3 (2000) A178-A179.

[12] S. Okada, S. Sawa, M. Egashira, J. Yamaki, M. Tabuchi, H. Kageyama, T. Konishi, A. Yoshino, J. Power Sources, 97-98 (2001) 430-432.

[13] N.N. Bramnik, K.G. Bramnik, T. Buhrmester, C. Baehtz, H. Ehrenberg, H. Fuess, J. Solid State Electrochem., 8 (2004) 558-564.

[14] J.M. Lloris, C. Pérez Vicente, J.L. Tirado, Electrochem. Solid-State Lett., 5 (2002) A234-A237.

[15] T. Gross, T. Buhrmester, K. Bramnik, N. Bramnik, K. Nikolowski, C. Baehtz, H. Ehrenberg, H. Fuess, Solid State Ionics (2004), accepted for publication.

[16] M. Knapp, V. Joco, C. Baehtz, H.H. Brecht, A. Berghaeuser, H. Ehrenberg, H. von Seggern, H. Fuess, Nucl Instrum Meth A, 521 (2004), 565.

[17] T. Roisnel, J. Rodriguez-Carvajal, (2002) WinPLOTR: a graphical tool for powder diffraction.

[18] A. Effekhari, J.Electrochem. Soc., 151 (2004) A1456-A1460.

[19] D. Morgan, A. Van der Ven and G. Geder, Electrochem. Solid-State Lett., 7 (2004), A30-A32

[20] M. Nakayama, S. Goto, Y. Uchimoto, M. Wakihara, Y. Kitajima, Chem. Mater., 16 (2004), 3399-3401.

[21] W.C. West, J.F. Whitacre, B.V. Ratnakumar, J.Electrochem. Soc., 150 (2003) A1660-A1666.

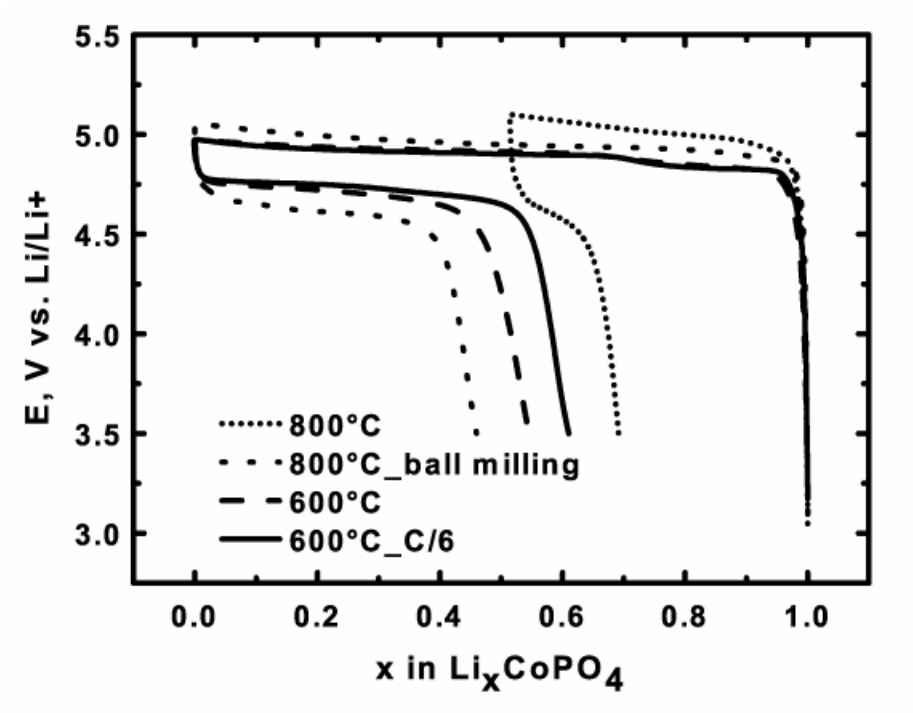

Fig.1. Galvanostatic charge-discharge curves for $LiCoPO_4$-based cathodes at rate C/1.5. $LiCoPO_4$ was prepared by "direct synthesis".

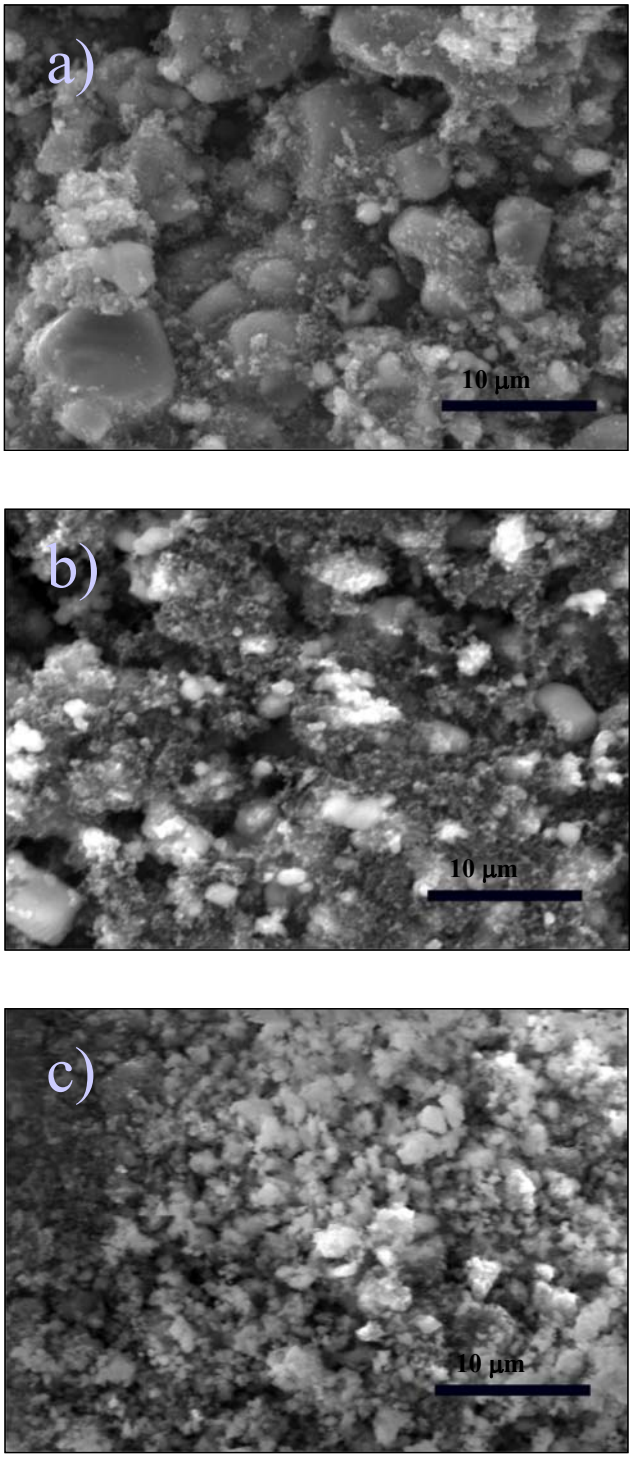

Fig.2. SEM micrograph showing the morphology of samples: a) annealed at 800°C, b) cathode mixture of the sample annealed at 800°C after ball-milling, c) annealed at 600°C. The whole section corresponds to an area of about 30µm×45 µm.

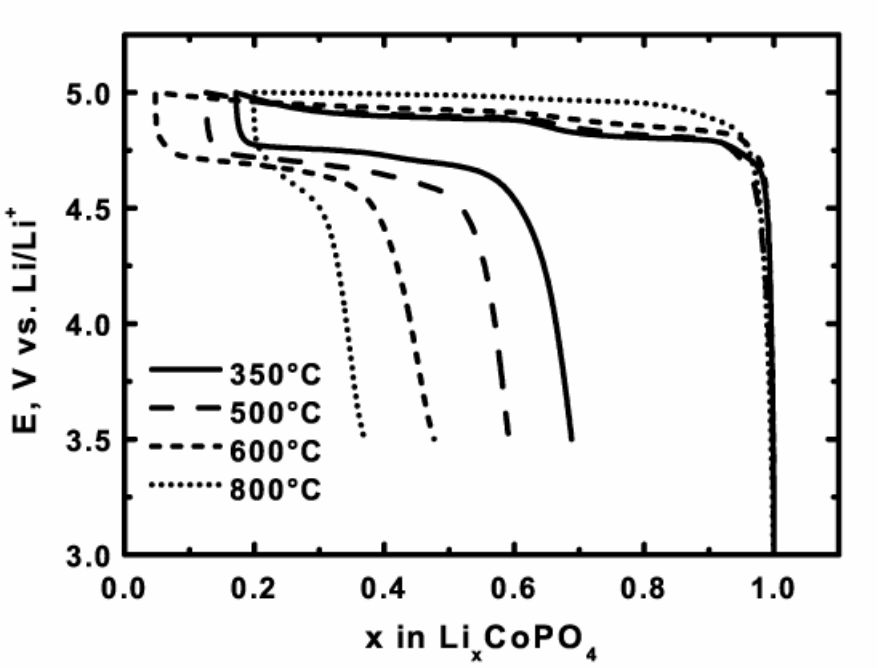

Fig. 3. First charge-discharge cycle for $LiCoPO_4$ prepared by "precursor" synthesis at different annealing temperatures (current rate close to C/1.5).

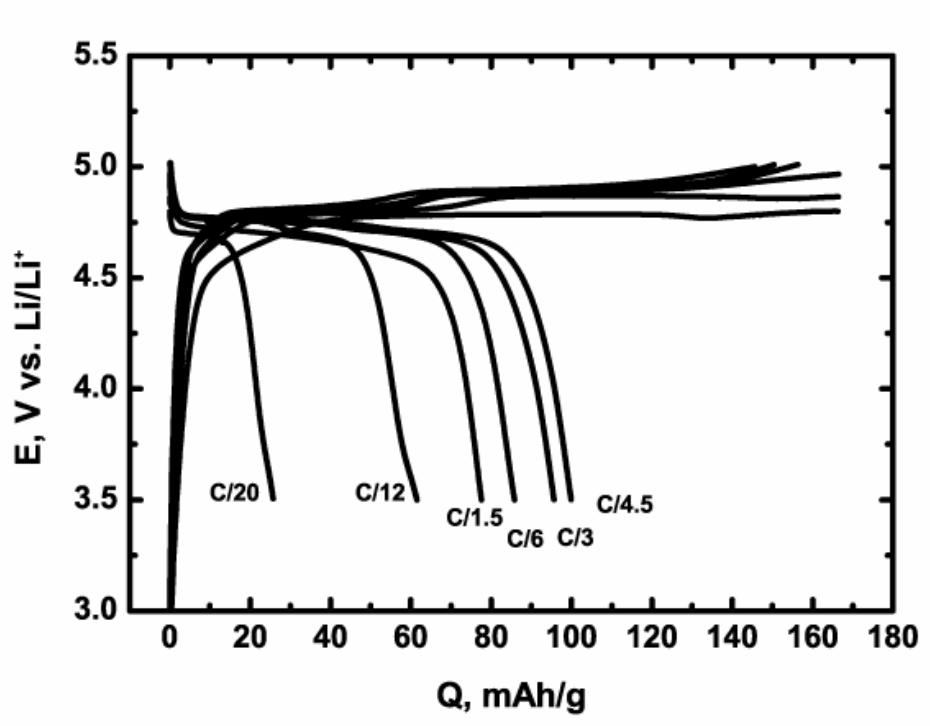

Fig.4. Rate capability of $LiCoPO_4$-cell ("precursor synthesis", annealed at 500°C).

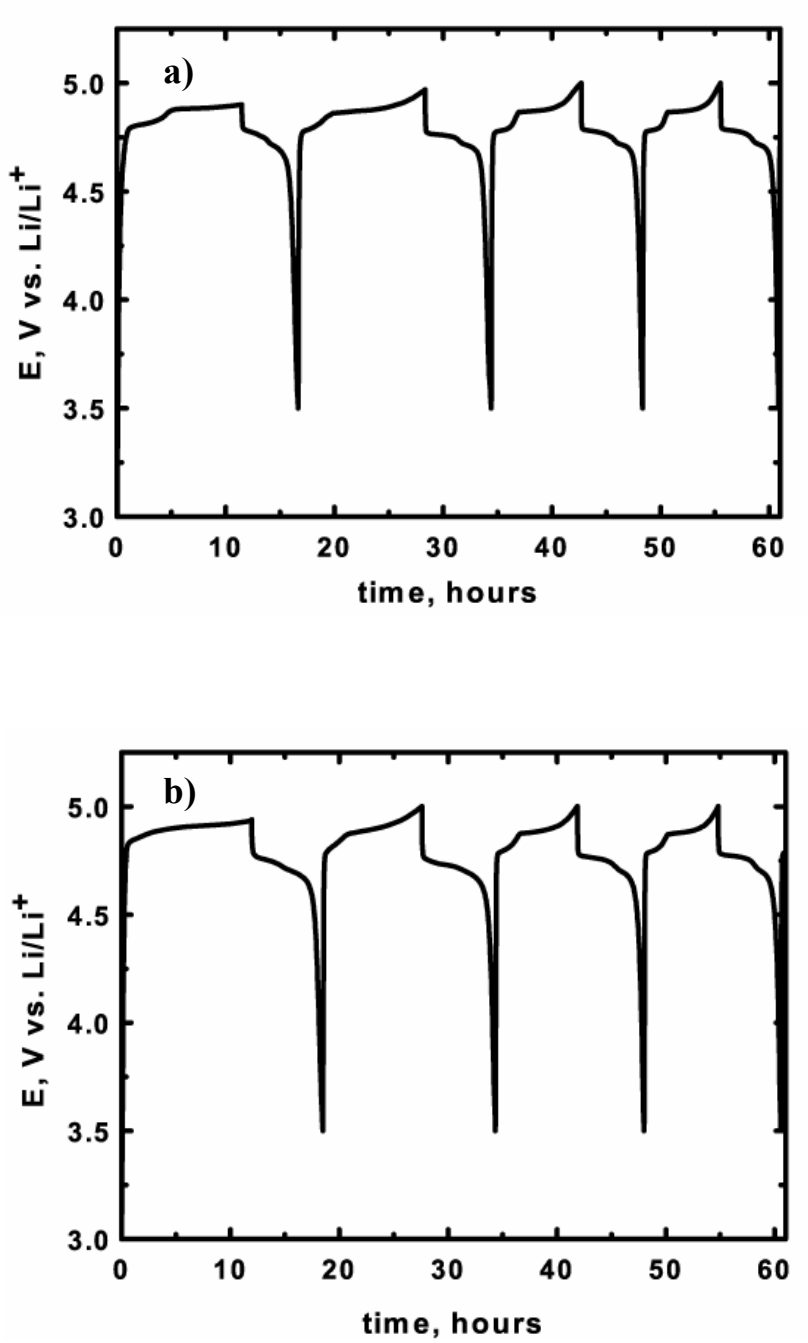

Fig. 5. E=f(t) curves obtained in potentiostatic mode at accelerating current close to C/13, a) $LiCoPO_4$-600°C b) $LiCoPO_4$-800°C, ball milled. Both samples were prepared by "direct synthesis".

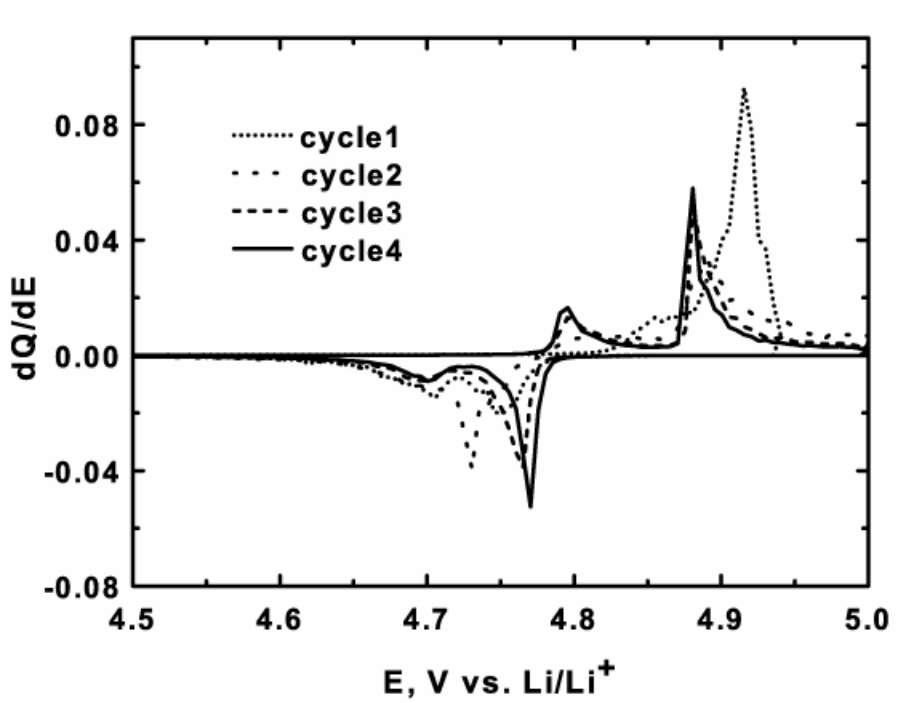

Fig.6. Incremental capacity plot for $LiCoPO_4$ annealed at 800°C ("direct synthesis") and ball-milled with carbon and PVdF for 15 minutes.

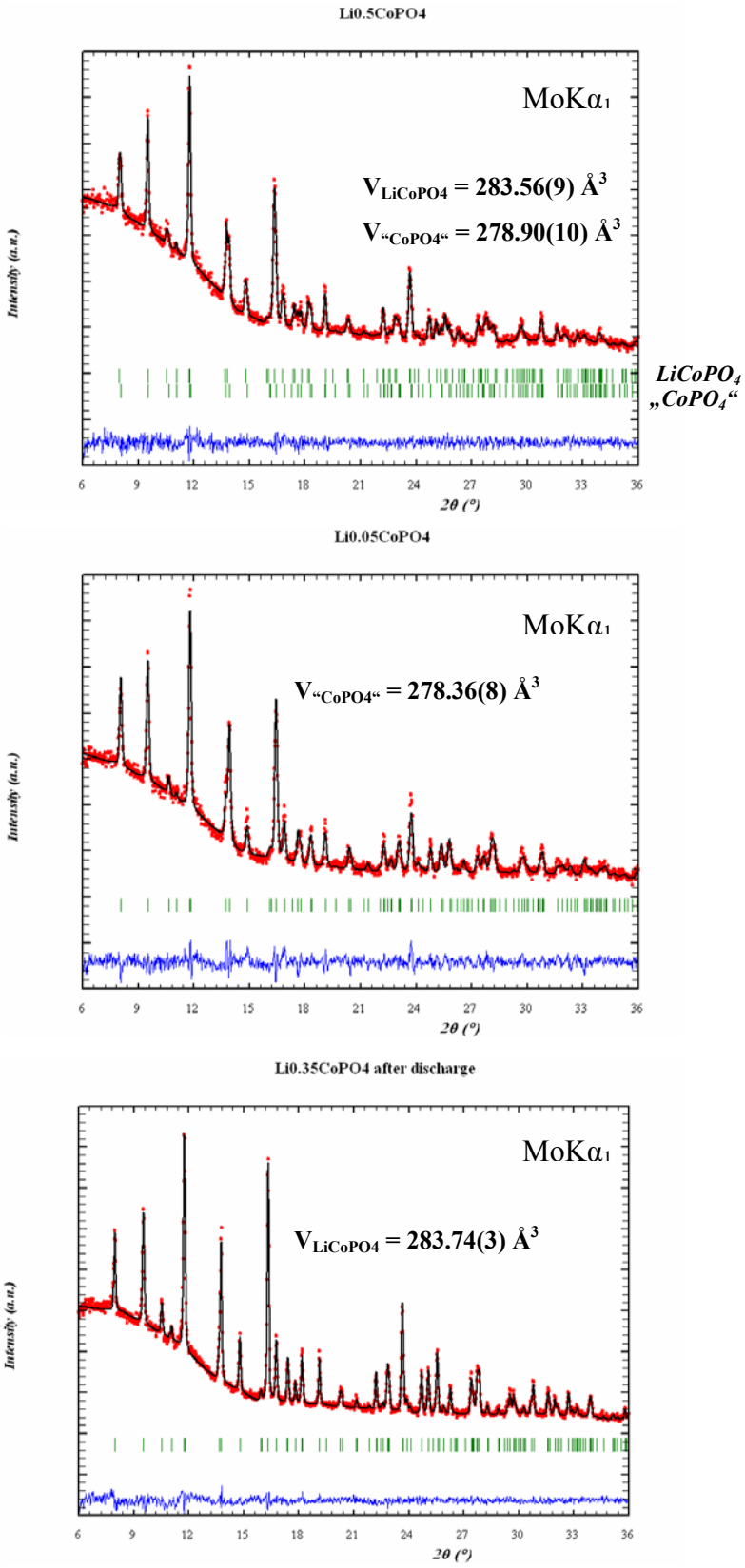

Fig.7. Ex-situ X-ray diffraction of the Li-deintercalated samples prepared from the $LiCoPO_4$ annealed at 800°C and ball-milled with carbon and PVdF for 15 minutes.

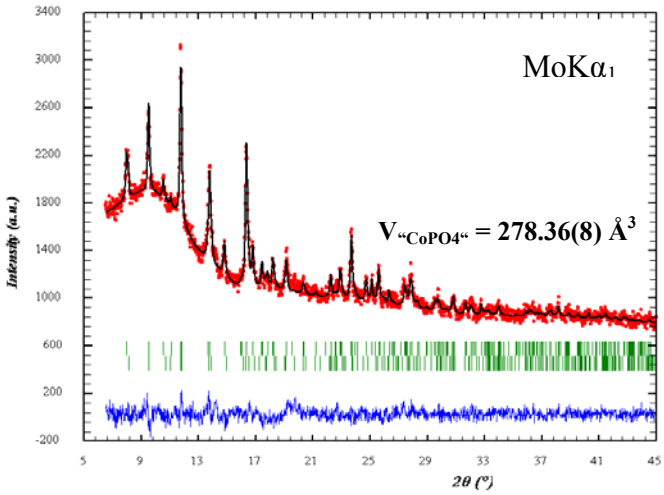

Fig. 8. X-ray diffraction pattern of the $Li_{0.05}CoPO_4$ sample ("direct" synthesis 600°C). Weight fractions of $LiCoPO_4$ and "$CoPO_4$" phase are of 85% and 15%, respectively.

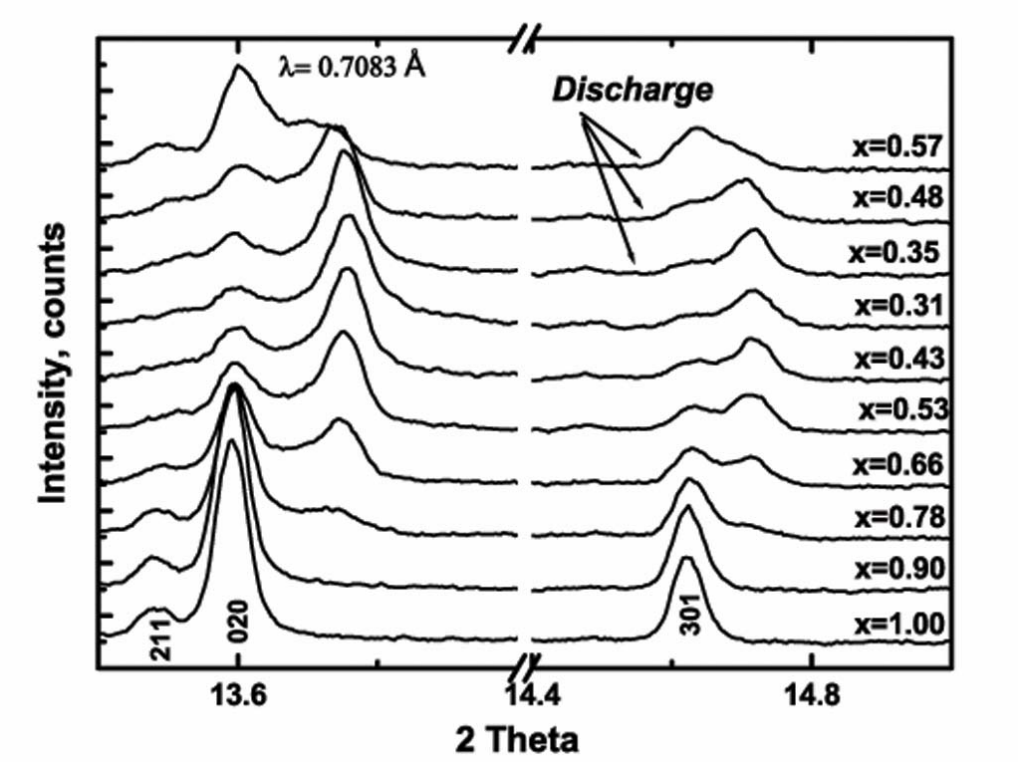

Fig. 9. Evolution of diffraction pattern during charge-discharge of the Li_xCoPO_4-cell ($LiCoPO_4$ annealed at 800°C and ball-milled with carbon and PVdF).

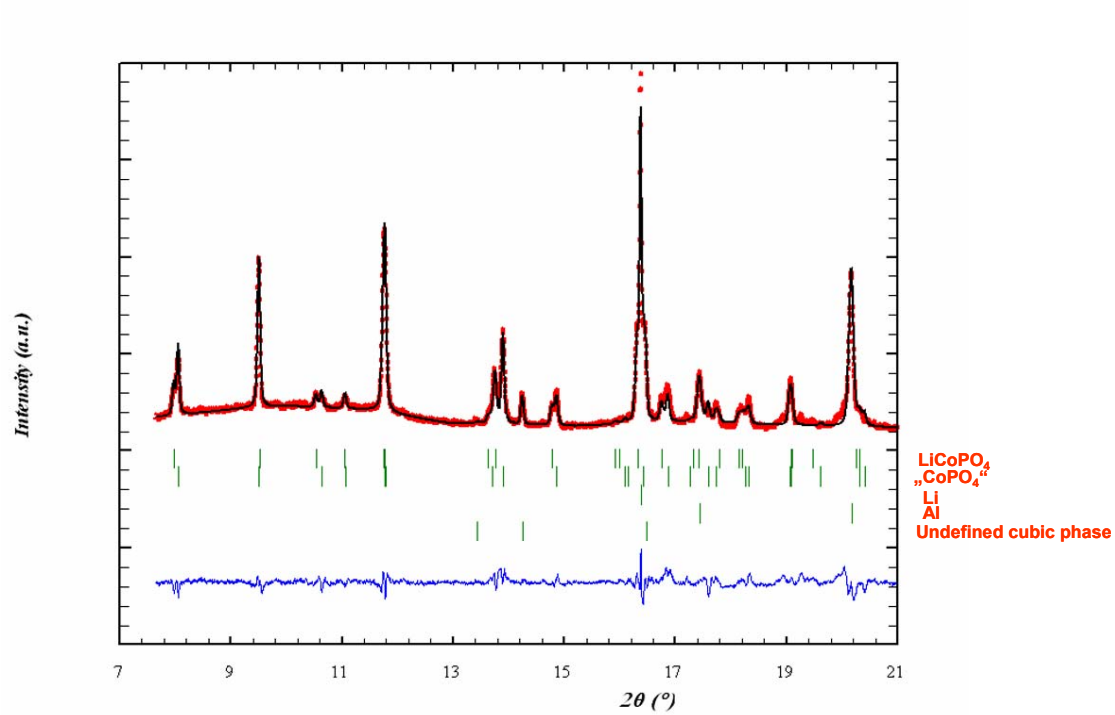

Fig.10. Synchrotron X-ray diffraction pattern taken in situ for $Li_{0.5}CoPO_4$ (λ= 0.70829 Å).

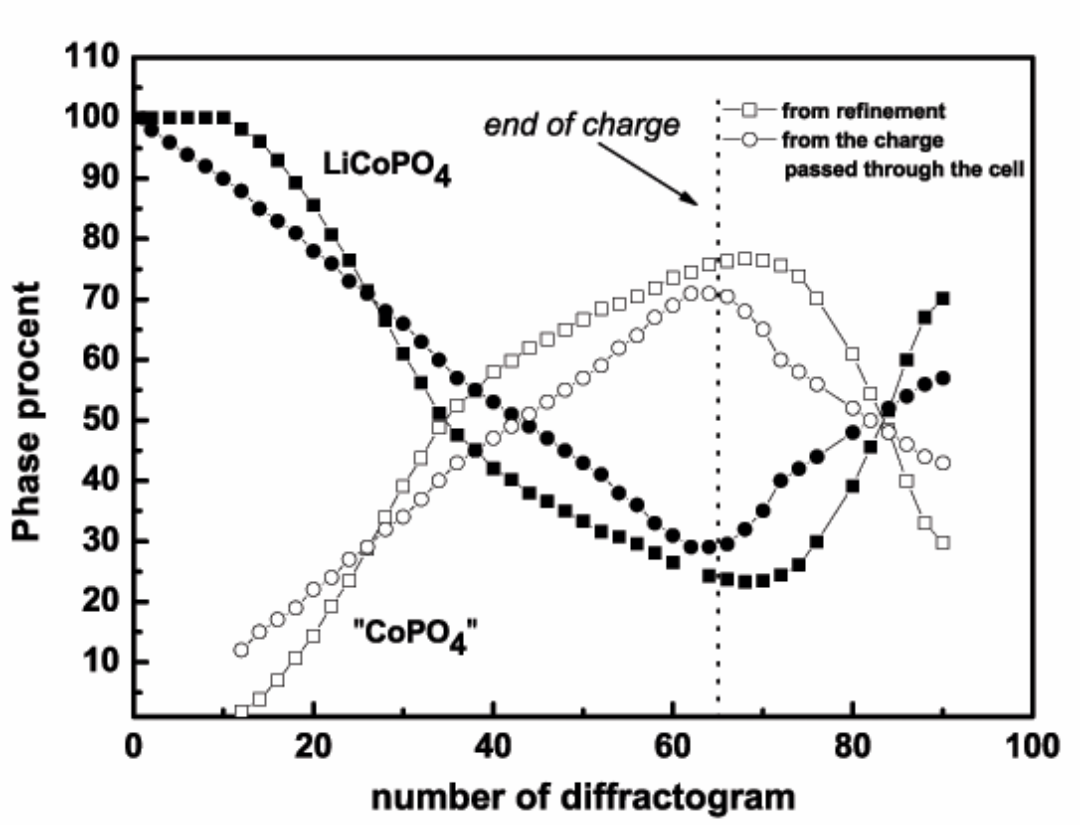

Fig. 11. Change in the phase ratios during charge-discharge, calculated from refinement versus electrochemical data. Filled circles and squares correspond to $LiCoPO_4$, empty ones – "$CoPO_4$".

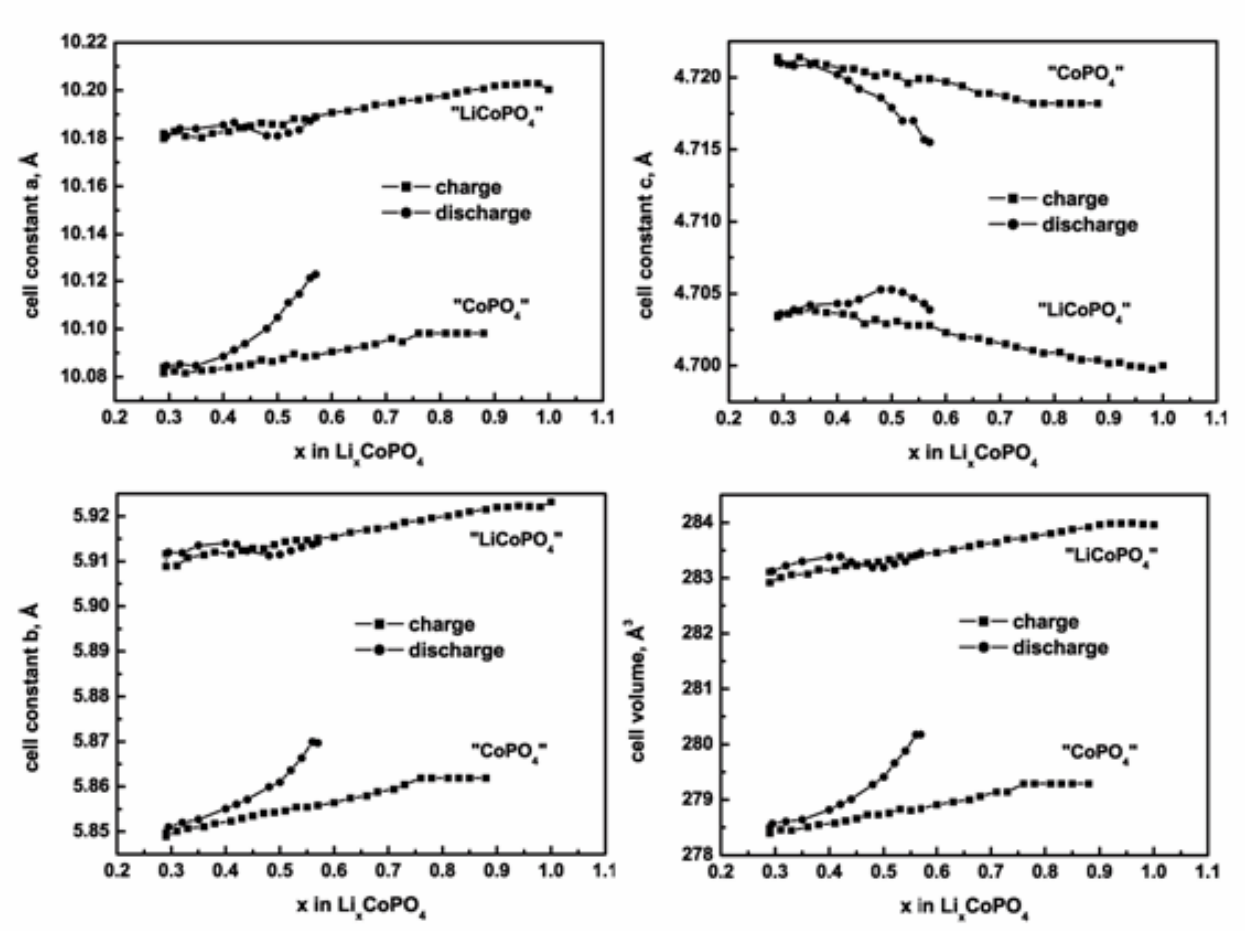

Fig. 12. Evolution of the cell parameters during charge-discharge of $LiCoPO_4$.